

Lawrence Berkeley National Laboratory

Climate & Ecosystems

Title

Functional roles of CymA and NapC in reduction of nitrate and nitrite by *Shewanella putrefaciens* W3-18-1

Permalink

<https://escholarship.org/uc/item/11s369ck>

Journal

Microbiology, 162(6)

ISSN

1350-0872

Authors

Wei, Hehong
Dai, Jingcheng
Xia, Ming
et al.

Publication Date

2016-06-01

DOI

10.1099/mic.0.000285

Peer reviewed

Functional roles of CymA and NapC in reduction of nitrate and nitrite by *Shewanella putrefaciens* W3-18-1

PDF

1.58 MB

HTML

101.19 Kb

- Authors: [Hehong Wei](#)^{1,2}, [Jingcheng Dai](#)¹, [Ming Xia](#)^{1,2}, [Margaret F. Romine](#)³, [Liang Shi](#)³, [Alex Beliy](#)³, [James M. Tiedje](#)⁴, [Kenneth H. Nealson](#)⁵, [James K. Fredrickson](#)³, [Jizhong Zhou](#)⁶, [Dongru Qiu](#)¹

-

- o [VIEW AFFILIATIONS](#)

- **Correspondence** Jizhong Zhou jzhou@ou.edu[Abstract](#)

- [Fulltext](#)

- [Figs \(7\)](#)

- [References \(50\)](#)

- [Cited By \(2\)](#)

- [Supplementary Material \(1\)](#)

- [Metrics](#)

- [Related Content](#)

INTRODUCTION

[GO TO SECTION...](#)

Most of the *Shewanella* strains display psychrophility or psychrotolerance as well as respiration flexibility and can utilize a series of substances including nitrate, nitrite, [Fe(III)] and manganese [Mn(III, IV)] (hydr)oxide sulphur compounds, heavy metals and metalloids, DMSO, and trimethylamine oxide (TMAO) for respiration ([Fredrickson et al., 2008](#) ; [Hau & Gralnick, 2007](#)). Comparative genomic analysis reveals that most *Shewanella* strains contain two types of periplasmic nitrate reductases (Nap), NapC-associated *nap-alpha* (*napEDABC*) and CymA-dependent *nap-beta* (*napDABGH*). The well-characterized *Shewanella oneidensis* MR-1 strain contains only *nap-beta* (*napDABGH*) for nitrate ammonification ([Chen et al., 2011](#) ; [Dong et al., 2012](#) ; [Simpson et al., 2010](#)) while the *Shewanella putrefaciens* W3-18-1 strain harbours both CymA- and NapC-dependent nitrate reductases, as well as the NapGH ubiquinol oxidase. These seemingly redundant respiratory chain components may be differentially expressed and

functioning under environmental condition gradients such as different oxygen tensions and availability of electron acceptors ([Qiu et al., 2013](#)).

NapC and CymA are both membrane-associated tetraheme cytochromes, and are similar in protein size and amino acid sequence ([Gescher et al., 2008](#) ; [Marriott et al., 2012a](#)). NapC and its homologues oxidize quinol in the cytoplasmic membrane and transfer the electrons released to their redox partners, such as nitrate reductase complex NapAB in the periplasm ([Berks et al., 1995](#) ; [Potter et al., 2001](#) ; [Roldan et al., 1998](#)). However, NapC is absent in *S. oneidensis* MR-1, and a possible less-specific homologous protein, CymA, is encoded. Moreover, it had been demonstrated previously that CymA is involved in reduction of iron(III), fumarate and nitrate ([Dong et al., 2012](#) ; [Fu et al., 2014](#) ; [Meyer et al., 2004](#) ; [Myers & Myers, 1997](#) , [2000](#)). More interestingly, NapC of *Escherichia coli* and CymA of *S. oneidensis* MR-1 had the same function under conditions of dissimilatory nitrate reduction ([Cruz-Garcia et al., 2007](#)). It was also shown that expression of *cymA* and *napC*, respectively, in conjunction with *fccA*, encoding the soluble fumarate reductase of *S. oneidensis* MR-1, could complement an *frdABCD* mutation in *E. coli*. Additionally and surprisingly, it was indicated that NapC, despite its 'specialized' function in the nitrate respiratory pathway, was functionally equivalent to CymA in its role *in vivo* as a soluble iron reductase, although at a lower rate ([Gescher et al., 2008](#)).

Thus, we proposed whether NapC and CymA in the *S. putrefaciens* W3-18-1 strain can function equivalently in nitrate reduction. As shown previously, CymA, a central part of electron transfer pathways that support respiratory flexibility of *Shewanella*, functions as an electron-transfer hub in anaerobic respiration ([Cordova et al., 2011](#) ; [Marriott et al., 2012a, b](#)). CymA can support the reduction of many electron acceptors, such as nitrate, nitrite, fumarate, DMSO, Fe³⁺, Mn⁴⁺, Cr⁴⁺ and arsenate ([Fonseca et al., 2013](#) ; [McMillan et al., 2012](#) ; [Murphy & Saltikov, 2007](#) ; [Szeinbaum et al., 2014](#)). Also, it has recently been shown that CymA is essential for selenite reduction by *S. oneidensis* MR-1 ([Li et al., 2014](#)). Our results indicated that NapC and CymA had no equivalent function in nitrate reduction, although both CymA and NapC can catalyse the same reaction transferring quinol-derived electrons to a periplasmic terminal reductase or an electron acceptor. NapC is only involved in nitrate reduction and can only interact specifically with Nap-alpha nitrate reductase, while CymA can interact promiscuously with Nap-alpha, Nap-beta and the NrfA nitrite reductase for nitrate and nitrite reduction. Moreover, site-directed mutagenesis was conducted to construct a series of NapC and CymA mutants for genetic complementation to probe their difference in specificity based on sequence alignment and a previous study ([Zargar & Saltikov, 2009](#)). It was found that the Lys-91, Asp-97 and Asp-166 residues of CymA play a key role in nitrate and nitrite reduction. Our results could provide insights into the molecular evolution of bacterial respiration in *Shewanella* and other bacteria.

METHODS

[GO TO SECTION...](#)

Bacterial strains and culture conditions.

S. putrefaciens W3-18-1 was usually cultured in Luria–Bertani (LB) broth or on LB plates at 28 °C (supplemented with 15 µg ml⁻¹ gentamycin and 50 µg ml⁻¹ kanamycin when necessary) ([Murray et al., 2001](#)). The microaerobic culture (without shaking) was conducted in modified M1 minimal medium ([Beliaev et al., 2005](#) ; [Myers & Nealson, 1988](#)) supplemented with 50 mM sodium lactate as carbon source and electron donor and 2 mM sodium nitrate or sodium nitrite as electron acceptor (supplemented with 50 µg ml⁻¹ kanamycin when necessary).

In-frame deletion.

By taking advantage of the easy genetic manipulation in the *S. putrefaciens* W3-18-1Δ *pstI*Δ *pstM* strain (Table S1, available in the online Supplementary Material) ([Qiu et al., 2013](#)), we generated a series of in-frame deletion mutants in this strain and tested their nitrate and nitrite reduction. The two-step protocol of selection (single crossover, antibiotic resistance) and counter-selection (double crossover, sucrose sensitivity) was applied for in-frame deletion of specific genes by using suicide vector pDS3.0 (R6K replicon, *sacB*, Gm^r, Table S1)-based constructs carrying a fusion of upstream and downstream sequences of target genes as described previously ([Wan et al., 2004](#)). The suicide vector was introduced into *S. putrefaciens* W3-18-1 by mating using *E. coli* WM3064 (Table S1) as the donor strain. Primers used are listed in Table S2.

Genetic complementation.

The plasmids pBBR1MCS-2- *cymA* and pBBR1MCS-2- *napC* were constructed for complementation analyses in the *S. putrefaciens* W3-18-1Δ *napC*Δ *cymA* double mutant (Table S1). PCR was used to amplify the *cymA* and *napC* genes from chromosomal DNA, and the PCR products were digested by using endonucleases *EcoRI* and *XbaI* and ligated into the digested broad-host-range plasmid pBBR1MCS-2 (Table S1, abbreviated as pBBR1-2 in the figures) ([Kovach et al., 1994](#) ; [Kovach & Peterson, 1995](#) ; [Pinchuk et al., 2009](#) ; [Wu et al., 2011](#)) to generate the constructs for genetic complementation. All the constructs were verified by PCR amplification, restriction mapping and sequencing. The resultant constructs were transferred into the *S. putrefaciens* W3-18-1Δ *napC*Δ *cymA* double mutant, respectively, via conjugation by using *E. coli* WM3064 as the donor. The transconjugants were selected by plating on LB agar supplemented with kanamycin and without diaminopimelic acids. Kanamycin-resistant colonies were streak-purified several times on LB agar plates containing kanamycin.

All mutated genes were cloned by using crossover PCR with appropriate primers. To clone those mutated genes, the ligation, verification, conjugation and selection were conducted as described above. To detect the expression of recombinant proteins, a His-tag was added to the C-terminal end of all genes. Primers used are listed in Table S2.

Western blot analysis.

Subcultures were grown in LB with 50 µg kanamycin ml⁻¹ at 28 °C and 220 r.p.m. for 8 h. The protein samples were then prepared by the standard procedures of the KeyGEN Biotech kit (KGP450, keyGEN). Proteins were analysed by 12 % SDS-PAGE and electro-transferred onto the 0.45 µm PVDF membrane in transfer buffer (47.8 mM Tris, 36.7 mM glycine, 1.3 mM SDS, 20 % (v/v) methanol). His-tagged proteins were probed with His monoclonal primary antibodies (Beyotime) at 1 : 1000 dilution and immuno-coupled with anti-Mouse IgG (H+L)-HRP (Beyotime)

according to the manufacturer's instructions. ECL Plus (Biosharp) was used for detection, and film images were digitized using ImageQuant LAS4000mini. The PVDF membrane stained with Coomassie brilliant blue after imaging was used as a loading control in the Western blot analysis ([Gilda & Gomes, 2013](#) ; [Welinder & Ekblad, 2011](#)).

Heme staining.

Subcultures were grown in LB with 50 µg kanamycin ml⁻¹ at 28 °C and 220 r.p.m. for 12 h. To detect CymA and NapC proteins, cells were centrifuged and resuspended in SDS loading buffer. The samples were separated by 18 % SDS-PAGE after being boiled and centrifuged. Heme stains were performed using 3,3',5,5'-tetramethylbenzidine (TMBZ) as previously described by [Francis & Becker, \(1984\)](#) and [Thomas et al.\(1976\)](#)).

Reduction of nitrate and nitrite.

In *S. putrefaciens* W3-18-1, nitrite can only be produced from nitrate by NAP nitrate reductases or from nitroalkane by 2-nitropropane dioxygenase (*Sputw3181_0570*). Thus, the changes of the nitrate and nitrite in the medium can be an indication of dissimilatory nitrate and nitrite reduction in modified M1 minimal medium without nitroalkane. The concentration of nitrate and nitrite in the medium was measured simultaneously by using a standard colorimetric method ([China EPA, 2002](#) ; [Nicholas & Nason, 1957](#)).

RNA extraction, reverse-transcription (RT)-PCR and real-time PCR analysis of gene transcription.

Total RNA was extracted by using the standard procedures of RNAiso Plus (Takara). The integrity of RNA was evaluated by agarose (1 %) gel electrophoresis. To prepare cDNA, 2 µg total RNA was reversely transcribed using a PrimeScript RT reagent Kit with gDNA Eraser (Takara) according to the manufacturer's protocol. Real-time PCR was then carried out with SYBR Premix Ex TaqII (Tli RNaseH Plus, Takara) on a Real-Time PCR System Light Cycler 480II(Roche). The relative mRNA levels were determined by normalization to the expression of 16S rRNA transcript ([Livak & Schmittgen, 2001](#) ; [Schmittgen & Livak, 2008](#)).

Meanwhile, RT-PCR was conducted with the same cDNA. The PCR thermal cycles were: 5 min at 95 °C for cDNA denaturation, followed by 27–30 cycles of 30 s at 95 °C, 30 s at 55 °C and 30 s at 72 °C. A final elongation step was performed for 10 min at 72 °C. RT-PCR products were separated on a 1 % agarose gel containing ethidium bromide and visualized by ultraviolet light and BioRad Image software. The data presented were relative mRNA levels normalized against 16S rRNA transcript levels, and the value of the control was set to 1.

All the experiments described were performed in triplicate to obtain means and SD. The PCR products were also sequenced to confirm amplification of target genes. Primers used are listed in Table S2.

RESULTS

[GO TO SECTION...](#)

Sequential reduction of nitrate and nitrite and diauxic growth

The well-studied *S. oneidensis* MR-1 strain conducts dissimilatory respiratory nitrate ammonification and exhibits sequential reduction of nitrate to nitrite and then to ammonium under anaerobic nitrate reduction conditions ([Cruz-Garcia et al., 2007](#) ; [Gao et al., 2009](#)). We also monitored the temporal changes of nitrate, nitrite and ammonium levels over the course of nitrate ammonification by both *S. putrefaciens* W3-18-1 and *S. putrefaciens* CN-32 strains. It was shown that nitrate was rapidly reduced into nitrite, which accumulated in the culture medium first before being further reduced into ammonium. The significant increase in ammonium levels coincided with the decrease in nitrite levels (Fig. S1, available in the online Supplementary Material). This two-step manner of nitrate ammonification is consistent with previous findings in *S. oneidensis* MR-1 ([Cruz-Garcia et al., 2007](#)). In agreement with these measurements, bacterial growth of the *S. putrefaciens* W3-18-1 strain exhibited a diauxic pattern, which was more notable in the modified M1 minimal medium ([Fig. 1](#)). An obvious lag phase appeared during diauxic shift from utilization of nitrate to nitrite as the electron acceptor in the *S. putrefaciens* W3-18-1 culture grown in the minimal medium ([Fig. 1](#)).

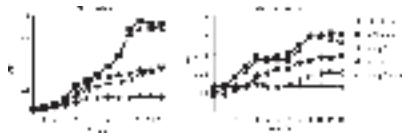


[Fig. 1.](#)

[Click to view](#)

Fig. 1.

Bacterial growth (OD₆₀₀) of wild-type *Shewanella putrefaciens* W3-18-1, in-frame deletion mutants $\Delta cymA$, $\Delta napC$ and $\Delta napC\Delta cymA$ double mutant on nitrate (2 mM) in the rich (1 % tryptone and 0.5 % yeast extract, w/v) and modified M1 minimal medium supplemented with 50 mM sodium lactate as electron donor and carbon source. The wild-type strain grown in culture medium without nitrate added was used as control.

NapC- and CymA-dependent nitrate reduction

The in-frame *cymA* (locus Sputw3181_3916) deletion mutant (Table S1) was generated in *S. putrefaciens* W3-18-1. It was shown that deletion of *cymA* led to significant decreases in reduction of ferric citrate (data not shown), suggesting that CymA plays a similar role in *S. putrefaciens* W3-18-1 as its ortholog in both *S. oneidensis* MR-1 and *Shewanella* sp. ANA-3 strains.

The in-frame *napC* deletion single mutant (Table S1) and the $\Delta napC\Delta cymA$ double mutant were also generated for exploring the functions of each gene. Deletion of *napC*, encoded within the *nap-alpha* operon, had no apparent effects on the bacterial growth on nitrate and the population growth also exhibited a diauxic pattern. On the other hand, the population growth and cell density of the *cymA* deletion mutant were significantly lower than those of the wild-type and *napC* mutant. The bacterial growth of the *cymA* mutant was still comparable with those of the wild-type and *napC* mutant in the initial stage (up to the sixth hour) corresponding to the stage of nitrate reduction, indicating that the nitrate reduction had not been severely

affected by deletion of *cymA*, and bacteria could no longer grow on nitrite in the absence of CymA. The deletion of both *napC* and *cymA* severely affected the bacterial growth on nitrate ([Fig. 1](#)), indicating that both of them were involved in nitrate reduction of *S. putrefaciens* W3-18-1. Time-course measurements of the nitrate and nitrite concentration in the culture broths also confirmed that nitrite was not further reduced to ammonium when *cymA* was deleted.

CymA and NapC do not function equivalently in nitrate reduction

A series of in-frame deletion mutants in *S. putrefaciens* W3-18-1 were generated and a series of constructs were constructed for genetic complementation analyses. By means of monitoring their nitrate and nitrite reduction in different test groups, it was demonstrated that CymA and NapC had no equivalent function in nitrate reduction. The results that the Napa with NapC in the $\Delta cymA\Delta nap\beta$ (Table S1) mutant could still reduce nitrate to nitrite and loss of CymA resulted in deficiency of nitrite reduction, and the $\Delta nap\beta\Delta napC$ (Table S1) mutant could still reduce nitrate and nitrite indicated that NapC could interact with Napa and CymA could interact with Napa and NrfA nitrite reductase ([Fig. 2a](#)). Moreover, NapC was unable to complement the nitrate reduction of the $\Delta cymA\Delta napa$ (Table S1) mutant and CymA could complement the nitrate and nitrite reduction of the $\Delta cymA\Delta napa$ mutant, which indicated that NapC was unable to interact with Nap β and NrfA nitrite reductase while CymA could interact with Nap β ([Fig. 2b](#)).

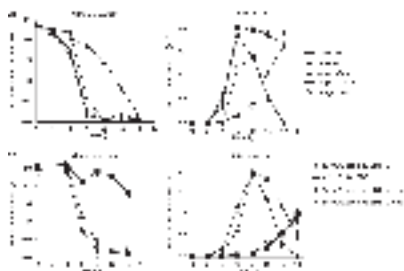


[Fig. 2.](#)

[Click to view](#)

Fig. 2.

CymA interacts with the nitrate reductases Napa and Nap β and the nitrite reductase NrfA and NapC only interacts with Napa. (a) The Napa with NapC in the $\Delta cymA\Delta nap\beta$ mutant can still reduce nitrate to nitrite and loss of CymA resulted in deficiency of nitrite reduction. (b) NapC was unable to complement the nitrate reduction of the $\Delta cymA\Delta napa$ mutant; CymA could complement the nitrate and nitrite reduction of the $\Delta cymA\Delta napa$ mutant. The error bars represent SD.

Western blot and heme staining analyses on CymA recombinant proteins

We hypothesized that the specificity of NapC and the promiscuity of CymA in the nitrate and nitrite reduction may depend on differences in both polypeptide sequence and structure. Sequence alignment between NapC and CymA revealed the CymA-specific motif DPE (166–168) ([Fig. 3](#)); therefore, a series of site-directed mutants of the *cymA* gene were generated for genetic complementation analyses (Table S3). Moreover, the pBBR1MCS-2-*cymA*^{K91Q}, pBBR1MCS-2-*cymA*^{K96Q} and pBBR1MCS-2-*cymA*^{D97A} constructs (Table S3) were constructed

based on previous experimental and bioinformatics analyses ([Zargar & Saltikov, 2009](#)). To monitor whether the recombinant proteins were expressed in the *S. putrefaciens* W3-18-1Δ *napCΔ cymA* host strain, the C-terminus of each mutant was modified with a His-tag by recombinant technology. His-tagged CymA and NapC, expressed off the pBBR1MCS-2- *napC*-His and pBBR1MCS-2- *cymA*-His plasmids, functioned equivalently with the untagged wild-type cytochromes in the Δ *napCΔ cymA* double mutant, suggesting that His-tags had no effects on the cellular functions (Fig. S2). All the His-tagged recombinant proteins were detected by Western blot analyses using anti-His-tag antibodies. Significant bands were detected in the Δ *napCΔ cymA* strains carrying plasmid-borne *cymA* or its mutants, but not in the control strain carrying the empty pBBR1MCS-2 vector ([Fig. 4a](#)).

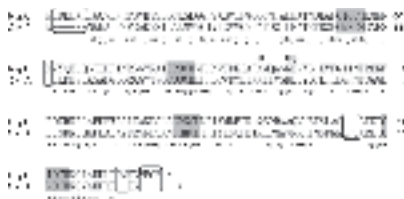


[Fig. 3.](#)

[Click to view](#)

Fig. 3.

Multiple sequence alignment of NapC and CymA revealed their specific amino acid residues (boxed). The D-166, P-167 and E-168 (boxed) of CymA, absent in NapC, may play a key role in the nitrate/nitrite reduction. K-91, K-96 and D-97 of CymA (arrow pointed) have been previously predicted to be the three sites involved in electron transfer. The heme-bound CXXCH motifs are highlighted in shadow. An * (asterisk) indicates positions which have a single, fully conserved residue. A : (colon) indicates conservation between groups of strongly similar properties. A . (full point) indicates conservation between groups of weakly similar properties.

As NapC and CymA are both tetraheme c-cytochromes, heme staining was used to detect the expression and maturation of various recombinant proteins. It was demonstrated that CymAΔDPE, CymAΔD166 and CymA^{D166A} proteins could hardly be detected in contrast to the other readily detectable CymA recombinant proteins by heme staining ([Fig. 4b](#)), suggesting that the Asp-166 residue of CymA may be crucial for the maturation of this tetraheme cytochrome.

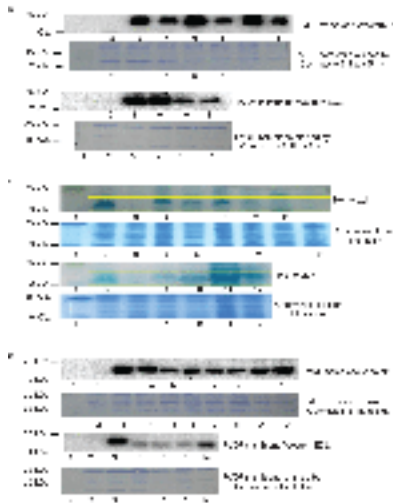


Fig. 4.

[Click to view](#)

Fig. 4.

(a) Western blot analyses on the expression of a series of plasmid-borne *cymA* and mutated *cymA* genes with the His-tag. Lane 1 is the size marker and lane 2 is the empty-vector-carrying $\Delta napC\Delta cymA$ double mutant used as negative control. Other lanes include His-tagged CymA (lane 3), CymA^{K91Q} (lane 4), CymA^{D97A} (lane 5), CymA^{D166A} (lane 6), CymA Δ D166 (lane 7), CymA Δ DPE (lane 8), CymA^{K96Q} (lane 9), CymA Δ P167 (lane 10) and CymA Δ E168 (lane 11) recombinant proteins detected by anti-His-tag antibody, respectively. (b) Heme staining analyses on the expression of a series of plasmid-borne *cymA* and mutated *cymA* genes. Lane 1 is the size marker, lane 2 is the empty-vector-carrying *S. putrefaciens* W3-18-1 wild-type strain as the positive control (untagged wild-type CymA) and lane 3 is the empty-vector-carrying $\Delta napC\Delta cymA$ double mutant used as the negative control. Other lanes include the His-tagged CymA (lane 4), His-tagged CymA^{K91Q} (lane 5), His-tagged CymA^{D97A} (lane 6), His-tagged CymA Δ DPE (lane 7), His-tagged CymA Δ D166 (lane 8), His-tagged CymA^{D166A} (lane 9), His-tagged CymA^{K96Q} (lane 10), His-tagged CymA Δ P167 (lane 11) and His-tagged CymA Δ E168 (lane 12) recombinant proteins expressed off plasmids in the double mutant and detected by TMBZ, respectively. (c) Western blot analyses on the expression of a series of plasmid-borne *napC* and mutated *napC* genes with the His-tag. Lane 1 is the size marker and lane 2 is the empty-vector-carrying $\Delta napC\Delta cymA$ double mutant used as negative control. Other lanes include His-tagged NapC (lane 3), NapC+DPE (lane 4), NapC+D (lane 5), NapC Δ LDKLLK (lane 6), NapC Δ N61 (lane 7), NapC Δ DM (lane 8), NapC Δ VEGF (lane 9), NapC^{E104D} (lane 10), NapC Δ LDKLLK Δ N Δ DM Δ VEGF (lane 11), NapC Δ LDKLLK Δ N Δ DM Δ VEGF^{E104D} (lane 12), NapC Δ LDKLLK Δ N Δ DM Δ VEGF+DPE (lane 13) and NapC Δ LDKLLK Δ N Δ DM Δ VEGF^{E104D}+DPE (lane 14) recombinant proteins detected by anti-His-tag antibody (upper panel), respectively.

Lys-91 and Asp-97 of CymA play a key role in nitrate reduction

All the CymA recombinant proteins were detected by Western blot, but CymA Δ DPE, CymA Δ D166 and CymA^{D166A} cytochromes were not detected by heme staining. Thus, it was concluded that the Asp-166 was a key site for maturation of CymA, which was consistent with the phenotypic observations that CymA Δ DPE, CymA Δ D166 and CymA^{D166A} were unable to

restore nitrate or nitrite reduction to the $\Delta napC\Delta cymA$ double mutant (Fig. S3). To verify the function of other sites, we tested whether the relevant mutants could restore nitrate or nitrite reduction to the $\Delta napC\Delta cymA$ double mutant. It was demonstrated that deletion of Pro-167 and Glu-168 had no effects on the function of CymA ([Table 1](#)). It was previously suggested that Lys-91 might be involved in the interaction of CymA with the quinol pool ([Zargar & Saltikov, 2009](#)) and substitution of Lys-91 with glutamine (Gln or Q) (designated $CymA^{K91Q}$) also resulted in the deficiency in both nitrate and nitrite reduction ([Fig. 5](#)). Furthermore, our finding that $CymA^{D97A}$ recombinant protein was deficient in nitrite reduction indicated that Asp-97 (corresponding to Glu-104 of NapC) might be the key factor determining electron transfer from CymA to NrfA and NapAB ([Fig. 6](#)). However, substitution of Lys-96 with Gln (Q) had no effects on the function of $CymA^{K96Q}$ in nitrate reduction ([Table 1](#)).

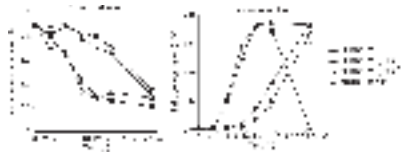


[Fig. 5.](#)

[Click to view](#)

Fig. 5.

Plasmid-borne $cymA^{K91Q}$ was unable to complement the nitrate reduction of the $\Delta napC\Delta cymA$ double mutant. The error bars represent SD .



[Fig. 6.](#)

[Click to view](#)

Fig. 6.

Plasmid-borne $cymA^{D97A}$ could complement nitrate reduction at a slower rate while it was unable to complement nitrite reduction. The error bars represent SD .

Click to view table

[Table 1.](#)

[Click to view](#)

Table 1. Phenotypes conferred to the *napC* and *cymA* double mutant by different constructs

Western blot and heme staining analyses on NapC recombinant proteins

Site-directed mutagenesis was conducted on the NapC of high specificity in interacting only with Nap-alpha. Sequence alignment between NapC and CymA revealed multiple NapC-specific amino acid residues and sequence motifs, including LDKLKK (residues 2–7), N61, DM (188–189) and the C-terminal VEGF (192–195) ([Fig. 3](#)). Therefore, a series of NapC mutants with deletion of those residues and motifs were generated (Table S3). Moreover, Glu-104(E) of NapC corresponded to the crucial residue Asp-97(D) of CymA as described above. We proposed that the *napC*^{E104D} mutation (Table S3) could result in a gain-of-function for nitrite reduction. Alternatively, it could be that the DPE (166–168) motif is CymA-specific and Asp-166 is crucial for the maturation of this tetraheme cytochrome. Therefore, a DPE motif or a D residue was inserted in between the Ser-170 and Gly-171 of NapC, corresponding to the same site of DPE located in CymA (Table S3). To modify NapC further, some other recombinant proteins (Table S3) were constructed with simultaneous deletion of multiple residues and motifs to make NapC closer to CymA.

As described above, Western blot and heme staining analyses were conducted to detect these recombinant NapC proteins. Our results indicated that CymA might be more stable than NapC because CymA was more readily detected (Fig. S4). Furthermore, it was more difficult to detect the NapCΔLDKLKKΔNΔDMΔVEGF polypeptide than the other NapC recombinant proteins ([Fig. 4c](#)). It is suggested that simultaneous deletion of the four NapC-specific motifs might have made the NapC mutant more unstable.

Site-directed mutagenesis on NapC

A series of mutants of *napC* was generated to test the functions of some NapC- and CymA-specific residues and motifs ([Fig. 3](#)). While the NapC mutants with deletion of the N61 residue, LDKLKK or VEGF motif could restore nitrate reduction to the Δ *napC*Δ *cymA* double mutant in a similar way to that of the wild-type, the mutant without the DM motif exhibited significantly reduced nitrate reduction (Fig. S5). Similarly, the substitution and addition of a CymA-specific residue and motifs to NapC, including NapC^{E104D}, NapC+D and NapC+DPE, still resulted in the same phenotype as NapC. In a word, those plasmid-borne *napC* mutants could still mediate nitrate reduction but conferred no nitrite reduction to the double mutant strain ([Table 1](#)).

However, the resultant *napC* mutant with simultaneous deletion of all four NapC-specific motifs (NapCΔLDK LKKΔNΔ DMΔVEGF) could complement neither nitrate reduction nor nitrite reduction in the Δ *napC*Δ *cymA* double mutant strain. Furthermore, the simultaneous deletion of NapC-specific motifs and addition of CymA-specific motifs (NapCΔLDKLKKΔNΔDMΔVEGF+DPE^{E104D}) conferred no nitrite reduction capacity to the NapC mutant (Fig. S6). These results were consistent with the Western blot results suggesting that these NapC-specific residues and motifs might play a key role in either electron transfer or protein stability but might not be related to the specificity of NapC. More efforts are needed in this gain-of-function approach to determine crucial amino acid residues and motifs for the specificity of NapC.

Crp regulates transcription of *cymA*

It is well established that Crp plays a crucial role in the regulation of anaerobic respiration in *S. oneidensis* MR-1, while this small regulatory protein regulates different cellular processes in closely related bacteria such as *E. coli* ([Saffarini et al., 2003](#)). The putative Crp binding site has been identified in the upstream of *napβ*, *nrfA* and *narQP* operons in *Shewanella loihica* PV-4, *S. oneidensis* MR-1 and *S. putrefaciens* W3-18-1 strains ([Dong et al., 2012](#); [Gao et al., 2010](#); [Qiu et al., 2013](#); [Stewart et al., 2009](#)). It has been previously confirmed that *napA* is independent of Crp-regulation ([Qiu et al., 2013](#)), and a putative Crp binding site was present upstream of *cymA* in *S. oneidensis* MR-1 and *S. putrefaciens* W3-18-1 strains (Fig. S7). The transcription levels of *napC* and *cymA* in the wild-type strain and the Δ *crp* mutant (Table S1) were analysed by using RT-PCR and real-time PCR. The expression of *cymA* decreased significantly in the the Δ *crp* mutant while *napC* transcription remained largely unchanged ([Fig. 7a, b](#)). These results are consistent with our previous finding that *napA* was independent of Crp regulation ([Qiu et al., 2013](#)). The expression of *cymA* is regulated by Crp in both *S. oneidensis* MR-1 and *S. putrefaciens* W3-18-1 strains.

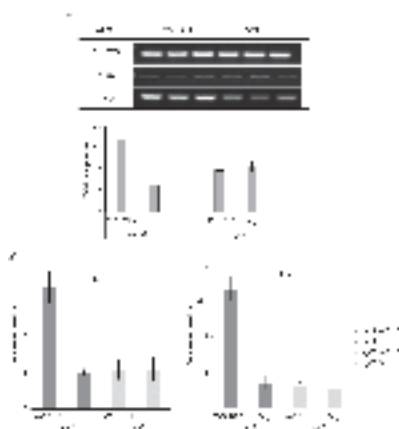


[Fig. 7.](#)

[Click to view](#)

Fig. 7.

Relative expression levels of the *napC* and *cymA* genes in the *S. putrefaciens* W3-18-1 wild-type strain and the Δ *crp* mutant by RT-PCR (a) and real-time PCR (b). Bacterial strains were cultured in modified M1 minimal medium supplemented with 50 mM sodium lactate as carbon source and electron donor and 2 mM sodium nitrate as electron acceptor without shaking. The data presented represent triplicate samples collected at 6 h and 8 h of incubation (mean \pm SD).

DISCUSSION

[GO TO SECTION...](#)

Sequential reduction of nitrate and nitrite

The two-step manner of nitrate ammonification may be common among the *Shewanella* strains. Previously it was proposed that the sequential reduction of nitrate and nitrite may be due to the oxygen sensitivity of nitrite reductase, which is normally expressed after the expression of nitrate reductase. However, the sole nitrate and nitrite reductases, NapA and NrfA, were simultaneously expressed in *S. oneidensis* MR-1 and it was argued that NapB helped to channel the CymA-mediated electron transport into NapA for nitrate reduction first because deletion of *napB* resulted in a coupled nitrate and nitrite reduction ([Gao et al., 2009](#)). On the other hand, it was elucidated that STC and FccA are necessary to bridge the periplasmic gap between the inner membrane-associated CymA and the outer membrane cytochromes in *S. oneidensis* MR-1 ([Schuetz et al., 2009](#) ; [Sturm et al., 2015](#)); the electron transfer direction may be regulated by these two electron-transfer hubs. Moreover, NMR analysis provides the opportunity to explore the dynamics of multidomain cytochromes and heme enzymes ([Neto et al., 2014](#)); the mechanism of the two-step reduction of nitrate and the difference of NapC and CymA in the interactions with NapAs and NrfA may be further explored this way.

The $\Delta napC\Delta cymA$ double mutant can still reduce nitrate to nitrite

A much slower nitrate reduction was observed in the $\Delta napC\Delta cymA$ double mutant because the concentration of nitrite in the medium slowly increased ([Fig. 4](#)). This suggests the existence of additional enzymes responsible for nitrate reduction in *S. putrefaciens* W3-18-1. *Shewanella* strains are well known for their respiration flexibility, owing largely to their numerous *c*-type cytochromes, many of which are uncharacterized functionally. Recently, it was reported that cytochrome *bc1* and CymA are functionally overlapping in nitrate/nitrite reduction in the *S. oneidensis* MR-1 strain ([Fu et al., 2013](#) , [2014](#)). Moreover, SirCD can replace CymA for respiration of fumarate, ferric citrate and DMSO in *S. oneidensis* MR-1 ([Cordova et al., 2011](#)). Therefore, other redox proteins may have functional similarity to that of CymA and NapC in terms of nitrate reduction in the *S. putrefaciens* W3-18-1 envelope.

Exploration of the functional sites in CymA and NapC

The *napC* gene is part of the *napEDABC* gene cluster, whereas *cymA* is a monocistronic gene in *Shewanella*. The NapC/NrfH family tetraheme cytochrome NrfH mediates the electron transfer from menaquinol to the nitrite reductase catalytic subunit (NrfA) of *Wolinella succinogenes* ([Simon et al., 2000](#)). Therefore, it was previously predicted that CymA might have derived from NrfH because CymA was required for nitrite reduction in *S. oneidensis* MR-1 ([Gao et al., 2009](#)). It had also been proposed that NapC might only participate in nitrate reduction, while CymA could play multiple roles in different electron transfer pathways ([Meyer et al., 2004](#)). Our analyses confirm that NapC is specific for nitrate reduction, while CymA is involved in reductions of nitrate as well as nitrite in *S. putrefaciens* W3-18-1.

Potential key amino acid residues of NapC and CymA were investigated, which may be attributed to the functional difference of these two members of the same protein family. Based on the alignment of their amino acid sequences and previous research, a series of mutants of NapC and CymA were generated to identify the loss-of-function mutations in *cymA* and gain-of-function mutations in *napC*. The Lys-91 residue was required for both nitrate and nitrite reduction, which is consistent with the previous finding that this residue is required for arsenate reduction and is probably crucial for quinol oxidation ([Zargar & Saltikov, 2009](#)). In addition, it

was found that the Asp-166 residue of CymA may play an important role in maturation of the cytochrome but is not involved in the specificity of CymA. However, it was found that the amino acid residue Asp-97 may be crucial for the functional diversity of CymA since the mutant CymA^{D97A} could still confer a nitrate reduction phenotype but not nitrite reduction. The nitrate reduction rate catalysed by this CymA mutant was slower than that of NapC, and the nitrite reduction was abolished. It is suggested that Asp-97 may facilitate the interaction of CymA with the cytochromes NapB and NrfA but not the NapA nitrate reductase.

Regulation and evolution of the Nap operons

It is usually considered that Nap α may be involved in denitrification or redox balancing and Nap β may serve in ammonification ([Simpson et al., 2010](#)). Moreover, previously, there was an evolutionary scenario of NAPs in *Shewanella*: Nap β as the prototype at the beginning, Nap α was subsequently obtained to form the dual NAP systems containing both Nap α and Nap β , which would finally evolve to a single Nap α ([Chenet et al., 2011](#)). It seems that the data presented in this paper and our previous analysis ([Qiu et al., 2013](#)) are consistent with this evolutionary scenario of the Naps. Nap α is independent of Crp regulation, and CymA, which is involved in the nitrate/nitrite reduction of Nap β , is Crp-regulated ([Figs 7 and S6](#)) ([Qiu et al., 2013](#)). Crp is a major regulator that plays an important role in cell division, starvation functions, motility and anaerobiosis ([Botsford & Harman, 1992](#) ; [Gao et al., 2010](#) ; [Saffarini et al., 2003](#)). Probably, the initial Crp-regulated Nap β can meet the needs for survival, and the concurrent Crp-independent Nap α may enhance the flexibility of *Shewanella* to diverse habitats. Nitrogen pollution has become increasingly severe, and therefore the Crp-independent Nap α required for denitrification may become the predominant functional cluster, whose expression is earlier than that of Nap β in *S. putrefaciens* W3-18-1 ([Qiu et al., 2013](#)).

ACKNOWLEDGEMENTS

[GO TO SECTION...](#)

This work was supported by the Chinese Academy of Science grant Y15103-1-401 and One-Hundred Scholar Award to D. Q. and the DOE grant DE-FG02-07ER64383 to J. Z.

REFERENCES

[GO TO SECTION...](#)

- **Beliaev A. S. , Klingeman D. M. , Klappenbach J. A. , Wu L. , Romine M. F. , Tiedje J. M. , Nealson K. H. , Fredrickson J. K. , Zhou J.** (2005). Global transcriptome analysis of *Shewanella oneidensis* MR-1 exposed to different terminal electron acceptors. *J Bacteriol* 187 7138–7145. [\[CrossRef\]](#) [\[PubMed\]](#) [\[Google Scholar\]](#)
- **Berks B. C. , Richardson D. J. , Reilly A. , Willis A. C. , Ferguson S. J.** (1995). The *napEDABC* gene cluster encoding the periplasmic nitrate reductase system of *Thiosphaera pantotropha* . *Biochem J* 309 983–992. [\[PubMed\]](#) [\[CrossRef\]](#) [\[Google Scholar\]](#)

- **Botsford J. L. , Harman J. G. (1992).** Cyclic AMP in prokaryotes. *Microbiol Rev* 56 100–122.[\[PubMed\]](#) [\[Google Scholar\]](#)
- **Chen Y. , Wang F. , Xu J. , Mehmood M. A. , Xiao X. (2011).** Physiological and evolutionary studies of NAP systems in *Shewanella piezotolerans* WP3. *ISME J* 5 843–855. [\[CrossRef\]](#) [\[PubMed\]](#) [\[Google Scholar\]](#)
- **China E P A. (2002).** *Water and Wastewater Monitoring Methods*. 4th edn, 266–274. Chinese Environmental Science Publishing House.[\[Google Scholar\]](#)
- **Cordova C. D. , Schicklberger M. F. , Yu Y. , Spormann A. M. (2011).** Partial functional replacement of CymA by SirCD in *Shewanella oneidensis* MR-1. *J Bacteriol* 193 2312–2321.[\[CrossRef\]](#) [\[PubMed\]](#) [\[Google Scholar\]](#)
- **Cruz-García C. , Murray A. E. , Klappenbach J. A. , Stewart V. , Tiedje J. M. (2007).** Respiratory nitrate ammonification by *Shewanella oneidensis* MR-1. *J Bacteriol* 189 656–662.[\[CrossRef\]](#) [\[PubMed\]](#) [\[Google Scholar\]](#)
- **Dong Y. , Wang J. , Fu H. , Zhou G. , Shi M. , Gao H. (2012).** A Crp-dependent two-component system regulates nitrate and nitrite respiration in *Shewanella oneidensis* . *PLoS One* 7 e51643.[\[CrossRef\]](#) [\[PubMed\]](#) [\[Google Scholar\]](#)
- **Fonseca B. M. , Paquete C. M. , Neto S. E. , Pacheco I. , Soares C. M. , Louro R. O. (2013).** Mind the gap: cytochrome interactions reveal electron pathways across the periplasm of *Shewanella oneidensis* MR-1 . *Biochem J* 449 101–108. [\[CrossRef\]](#) [\[PubMed\]](#) [\[Google Scholar\]](#)
- **Francis R. T. , Becker R. R. (1984).** Specific indication of hemoproteins in polyacrylamide gels using a double-staining process. *Anal Biochem* 136 509–514. [\[PubMed\]](#) [\[CrossRef\]](#) [\[Google Scholar\]](#)
- **Fredrickson , Romine M. F. , Beliaev A. S. , Auchtung J. M. , Driscoll M. E. , Gardner T. S. , Nealson K. H. , Osterman A. L. , Pinchuk G. , et al(2008).** Towards environmental systems biology of *Shewanella* . *Nat Rev Microbiol* 6 592–603. [\[CrossRef\]](#) [\[PubMed\]](#) [\[Google Scholar\]](#)
- **Fu H. , Chen H. , Wang J. , Zhou G. , Zhang H. , Zhang L. , Gao H. (2013).** Crp-dependent cytochrome *bd* oxidase confers nitrite resistance to *Shewanella oneidensis* . *Environ Microbiol* 15 2198–2212.[\[CrossRef\]](#) [\[PubMed\]](#) [\[Google Scholar\]](#)
- **Fu H. , Jin M. , Ju L. , Mao Y. , Gao H. (2014).** Evidence for function overlapping of CymA and the cytochrome *bc1* complex in the *Shewanella oneidensis* nitrate and nitrite respiration. *Environ Microbiol* 16 3181–3195.[\[CrossRef\]](#) [\[PubMed\]](#) [\[Google Scholar\]](#)
- **Gao H. , Wang X. , Yang Z. K. , Chen J. , Liang Y. , Chen H. , Palzkill T. , Zhou J. (2010).** Physiological roles of ArcA, Crp, and EtrA and their interactive control on aerobic and anaerobic respiration in *Shewanella oneidensis* . *PLoS One* 5 e15295.[\[CrossRef\]](#) [\[PubMed\]](#) [\[Google Scholar\]](#)
- **Gao H. , Yang Z. K. , Barua S. , Reed S. B. , Romine M. F. , Nealson K. H. , Fredrickson J. K. , Tiedje J. M. , Zhou J. (2009).** Reduction of nitrate in *Shewanella oneidensis* depends on atypical NAP and NRF systems with NapB as a preferred electron transport protein from CymA to NapA. *ISME J* 3 966–976.[\[CrossRef\]](#) [\[PubMed\]](#) [\[Google Scholar\]](#)

- **Gescher J. S. , Cordova C. D. , Spormann A. M.** (2008). Dissimilatory iron reduction in *Escherichia coli*: identification of CymA of *Shewanella oneidensis* and NapC of *E. coli* as ferric reductases. *Mol Microbiol* 68 706–719. [\[CrossRef\]](#) [\[PubMed\]](#) [\[Google Scholar\]](#)
- **Gilda J. E. , Gomes A. V.** (2013). Stain-free total protein staining is a superior loading control to β -actin for Western blots. *Anal Biochem* 440186–188. [\[CrossRef\]](#) [\[PubMed\]](#) [\[Google Scholar\]](#)
- **Hau H. H. , Gralnick J. A.** (2007). Ecology and biotechnology of the genus *Shewanella* . *Annu Rev Microbiol* 61 237–258. [\[CrossRef\]](#) [\[PubMed\]](#) [\[Google Scholar\]](#)
- **Kovach M. E. , Elzer P. H. , Hill D. S. , Robertson G. T. , Farris M. A. , Roop R. M. , Peterson K. M.** (1995). Four new derivatives of the broad-host-range cloning vector pBBR1MCS, carrying different antibiotic-resistance cassettes. *Gene* 166 175–176. [\[CrossRef\]](#) [\[PubMed\]](#) [\[Google Scholar\]](#)
- **Kovach M. E. , Phillips R. W. , Elzer P. H. , Roop R. M. , Peterson K. M.** (1994). pBBR1MCS: a broad-host-range cloning vector. *Biotechniques* 16800–802. [\[PubMed\]](#) [\[Google Scholar\]](#)
- **Li D.-B. , Cheng Y.-Y. , Wu C. , Li W.-W. , Li N. , Yang Z.-C. , Tong Z.-H. , Yu H.-Q.** (2014). Sel enite reduction by *Shewanella oneidensis* MR-1 is mediated by fumarate reductase in periplasm. *Sci Rep* 4 [\[PubMed\]](#) [\[Google Scholar\]](#)
- **Livak K. J. , Schmittgen T. D.** (2001). Analysis of relative gene expression data using real-time quantitative PCR and the $2^{-\Delta\Delta C(T)}$ method. *Methods* 25 402–408. [\[CrossRef\]](#) [\[PubMed\]](#) [\[Google Scholar\]](#)
- **Marritt S. J. , Lowe T. G. , Bye J. , McMillan D. G. G. , Shi L. , Fredrickson J. , Zachara J. , Richardson D. J. , Cheesman M. R. , et al** (2012a). A functional description of CymA, an electron-transfer hub supporting anaerobic respiratory flexibility in *Shewanella* . *Biochem J* 444 465–474. [\[CrossRef\]](#) [\[Google Scholar\]](#)
- **Marritt S. J. , McMillan D. G. G. , Shi L. , Fredrickson J. K. , Zachara J. M. , Richardson D. J. , Jeuken L. J. C. , Butt J. N.** (2012b). The roles of cyma in support of the respiratory flexibility of *shewanella oneidensis* MR-1. *Biochem Soc T* 40 1217–1221. [\[CrossRef\]](#) [\[Google Scholar\]](#)
- **McMillan D. G. , Marritt S. J. , Butt J. N. , Jeuken L. J.** (2012). Menaquinone-7 is specific cofactor in tetraheme quinol dehydrogenase CymA. *J Biol Chem* 287 14215–14225. [\[CrossRef\]](#) [\[PubMed\]](#) [\[Google Scholar\]](#)
- **Meyer T. E. , Tsapin A. I. , Vandenberghe I. , de Smet L. , Frishman D. , Neilson K. H. , Cusanovich M. A. , van Beeumen J. J.** (2004). Identification of 42 possible cytochrome C genes in the *Shewanella oneidensis* genome and characterization of six soluble cytochromes. *OMICS* 8 57–77. [\[CrossRef\]](#) [\[PubMed\]](#) [\[Google Scholar\]](#)
- **Murphy J. N. , Saltikov C. W.** (2007). The *cymA* gene, encoding a tetraheme c-type cytochrome, is required for arsenate respiration in *Shewanella* species. *J Bacteriol* 189 2283–2290. [\[CrossRef\]](#) [\[PubMed\]](#) [\[Google Scholar\]](#)

- **Murray A. E. , Lies D. , Li G. , Neilson K. , Zhou J. , Tiedje J. M.** (2001). DNA/DNA hybridization to microarrays reveals gene-specific differences between closely related microbial genomes. *P Natl Acad Sci USA* 98 9853–9858. [\[CrossRef\]](#) [\[Google Scholar\]](#)
- **Myers C. R. , Myers J. M.** (1997). Cloning and sequence of *cymA*, a gene encoding a tetraheme cytochrome C required for reduction of iron(III), fumarate, and nitrate by *Shewanella putrefaciens* MR-1. *J Bacteriol* 179 1143–1152. [\[PubMed\]](#) [\[Google Scholar\]](#)
- **Myers C. R. , Neilson K. H.** (1988). Bacterial manganese reduction and growth with manganese oxide as the sole electron acceptor. *Science* 240 1319–1321. [\[CrossRef\]](#) [\[PubMed\]](#) [\[Google Scholar\]](#)
- **Myers J. M. , Myers C. R.** (2000). Role of the tetraheme cytochrome CymA in anaerobic electron transport in cells of *Shewanella putrefaciens* MR-1 with normal levels of menaquinone. *J Bacteriol* 182 67–75. [\[PubMed\]](#) [\[CrossRef\]](#) [\[Google Scholar\]](#)
- **Neto S. E. , Fonseca B. M. , Maycock C. , Louro R. O.** (2014). Analysis of the residual alignment of a paramagnetic multiheme cytochrome by NMR. *Chem Commun (Camb)* 50 4561–4563. [\[CrossRef\]](#) [\[PubMed\]](#) [\[Google Scholar\]](#)
- **Nicholas D. J. D. , Nason A.** (1957). Determination of nitrate and nitrite. *Method Enzymol* 3 981–984. [\[CrossRef\]](#) [\[Google Scholar\]](#)
- **Pinchuk G. E. , Rodionov D. A. , Yang C. , Li X. , Osterman A. L. , Dervyn E. , Geydebrekht O. V. , Reed S. B. , Romine M. F. , et al** (2009). Genomic reconstruction of *Shewanella oneidensis* MR-1 metabolism reveals a previously uncharacterized machinery for lactate utilization. *P Natl Acad Sci* 106 2874–2879. [\[CrossRef\]](#) [\[Google Scholar\]](#)
- **Potter L. , Angove H. , Richardson D. , Cole J.** (2001). Nitrate reduction in the periplasm of gram-negative bacteria. *Adv Microb Physiol* 4551–112. [\[PubMed\]](#) [\[CrossRef\]](#) [\[Google Scholar\]](#)
- **Qiu D. , Wei H. , Tu Q. , Yang Y. , Xie M. , Chen J. , Pinkerton M. H., Jr. , Liang Y. , He Z. , Zhou J** (2013). Combined genomics and experimental analyses of respiratory characteristics of *Shewanella putrefaciens* W3-18-1. *Appl Environ Microbiol* 79 5250–5257. [\[CrossRef\]](#) [\[PubMed\]](#) [\[Google Scholar\]](#)
- **Roldán M. D. , Sears H. J. , Cheesman M. R. , Ferguson S. J. , Thomson A. J. , Berks B. C. , Richardson D. J.** (1998). Spectroscopic characterization of a novel multiheme c-type cytochrome widely implicated in bacterial electron transport. *J Biol Chem* 273 28785–28790. [\[PubMed\]](#) [\[CrossRef\]](#) [\[Google Scholar\]](#)
- **Saffarini D. A. , Schultz R. , Beliaev A.** (2003). Involvement of cyclic AMP (cAMP) and cAMP receptor protein in anaerobic respiration of *Shewanella oneidensis* . *J Bacteriol* 185 3668–3671. [\[PubMed\]](#) [\[CrossRef\]](#) [\[Google Scholar\]](#)
- **Schmittgen T. D. , Livak K. J.** (2008). Analyzing real-time PCR data by the comparative C(T) method. *Nat Protoc* 3 1101–1108. [\[PubMed\]](#) [\[CrossRef\]](#) [\[Google Scholar\]](#)
- **Schuetz B. , Schicklberger M. , Kuermann J. , Spormann A. M. , Gescher J.** (2009). Periplasmic electron transfer via the c-type cytochromes MtrA and FccA of *Shewanella oneidensis* MR-1. *Appl Environ Microbiol* 75 7789–7796. [\[CrossRef\]](#) [\[PubMed\]](#) [\[Google Scholar\]](#)

- **Simon J. , Gross R. , Einsle O. , Kroneck P. M. , Kröger A. , Klimmek O. (2000).** A NapC/NirT-type cytochrome c (*NrfH*) is the mediator between the quinone pool and the cytochrome c nitrite reductase of *Wolinella succinogenes* . *Mol Microbiol* 35 686–696. [\[PubMed\]](#) [\[CrossRef\]](#) [\[Google Scholar\]](#)
- **Simpson P. J. , Richardson D. J. , Codd R. (2010).** The periplasmic nitrate reductase in *Shewanella*: the resolution, distribution and functional implications of two NAP isoforms, NapEDABC and NapDAGHB. *Microbiology* 156 302–312. [\[CrossRef\]](#) [\[PubMed\]](#) [\[Google Scholar\]](#)
- **Stewart V. , Bledsoe P. J. , Chen L. L. , Cai A. (2009).** Catabolite repression control of *napF* (periplasmic nitrate reductase) operon expression in *Escherichia coli* K-12. *J Bacteriol* 191 996–1005. [\[CrossRef\]](#) [\[PubMed\]](#) [\[Google Scholar\]](#)
- **Sturm G. , Richter K. , Doetsch A. , Heide H. , Louro R. O. , Gescher J. (2015).** A dynamic periplasmic electron transfer network enables respiratory flexibility beyond a thermodynamic regulatory regime. *ISME J* 9 1802–1811. [\[CrossRef\]](#) [\[PubMed\]](#) [\[Google Scholar\]](#)
- **Szeinbaum N. , Burns J. L. , DiChristina T. J. (2014).** Electron transport and protein secretion pathways involved in Mn(III) reduction by *Shewanella oneidensis*. *Env Microbiol Rep* 6 490–500. [\[CrossRef\]](#) [\[Google Scholar\]](#)
- **Thomas P. E. , Ryan D. , Levin W. (1976).** An improved staining procedure for the detection of the peroxidase activity of cytochrome P-450 on sodium dodecyl sulfate polyacrylamide gels. *Anal Biochem* 75 168–176. [\[PubMed\]](#) [\[CrossRef\]](#) [\[Google Scholar\]](#)
- **Wan X. F. , Verberkmoes N. C. , McCue L. A. , Stanek D. , Connelly H. , Hauser L. J. , Wu L. , Liu X. , Yan T. , *et al* (2004).** Transcriptomic and proteomic characterization of the Fur modulon in the metal-reducing bacterium *Shewanella oneidensis* . *J Bacteriol* 186 8385–8400. [\[CrossRef\]](#) [\[PubMed\]](#) [\[Google Scholar\]](#)
- **Welinder C. , Ekblad L. (2011).** Coomassie staining as loading control in Western blot analysis. *J Proteome Res* 10 1416–1419. [\[CrossRef\]](#) [\[PubMed\]](#) [\[Google Scholar\]](#)
- **Wu L. , Wang J. , Tang P. , Chen H. , Gao H. (2011).** Genetic and molecular characterization of flagellar assembly in *Shewanella oneidensis* . *PLoS One* 6 e21479. [\[CrossRef\]](#) [\[PubMed\]](#) [\[Google Scholar\]](#)
- **Zargar K. , Saltikov C. W. (2009).** Lysine-91 of the tetraheme c-type cytochrome CymA is essential for quinone interaction and arsenate respiration in *Shewanella* sp. strain ANA-3. *Arch Microbiol* 191 797–806. [\[CrossRef\]](#) [\[PubMed\]](#) [\[Google Scholar\]](#)